

# Thermal Biophysics Lectures

Rajiv Chopra

[chopra@sri.utoronto.ca](mailto:chopra@sri.utoronto.ca)

Rm C713, Imaging Research

Sunnybrook Health Sciences Centre

2075 Bayview Avenue, Toronto, Ontario, M4N3M5

# Big Picture

- Lecture 1: Biology/Rationale/Nomenclature
- Lecture 2: Blood Flow/Modelling
- **Lecture 3: Energy Delivery**
- Lecture 4: Thermometry/Treatment monitoring

# Review

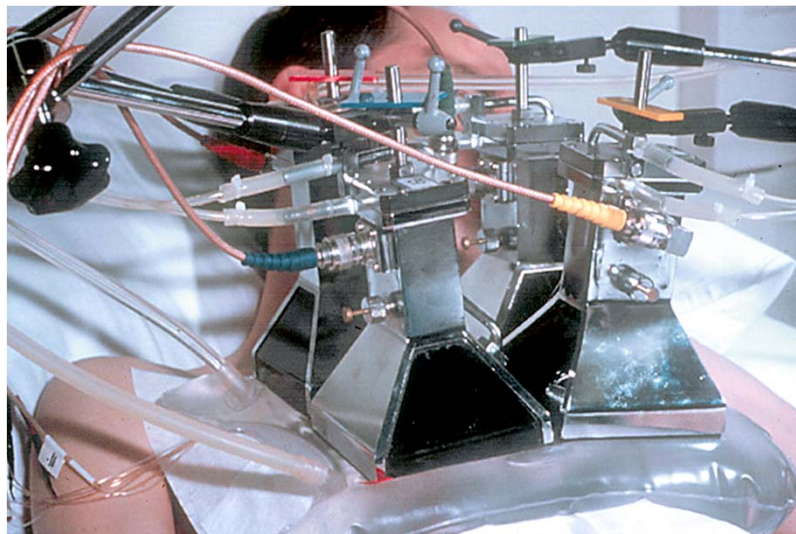
- Key physical/biological concepts in thermal therapy
- Arrhenius Models of Heat-Induced Cell Killing & Thermal Dose (Cell Survival Curves)
- Thermotolerance & heat shock proteins
- Bioheat Transfer Equation for modelling
- Response of blood flow during heating in normal tissue and tumours

# This Lecture

- Discuss different forms of energy delivery for thermal therapy
  - Hyperthermia & high temperature thermal therapy
  - EM devices, Ultrasound devices

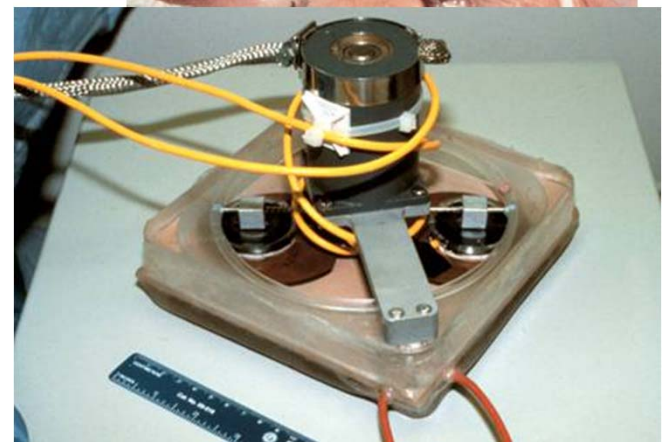
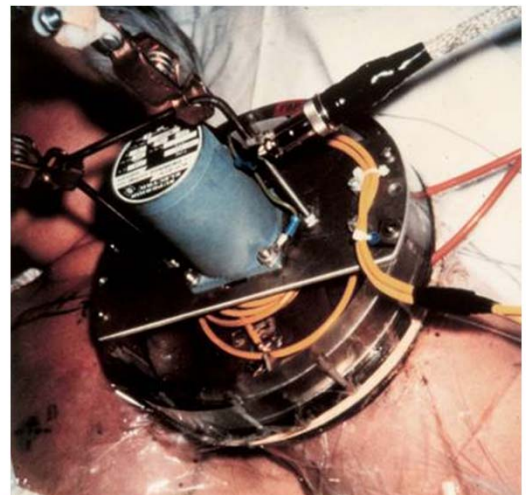
# **TECHNIQUES FOR ENERGY DELIVERY**

# Many approaches have been tried...

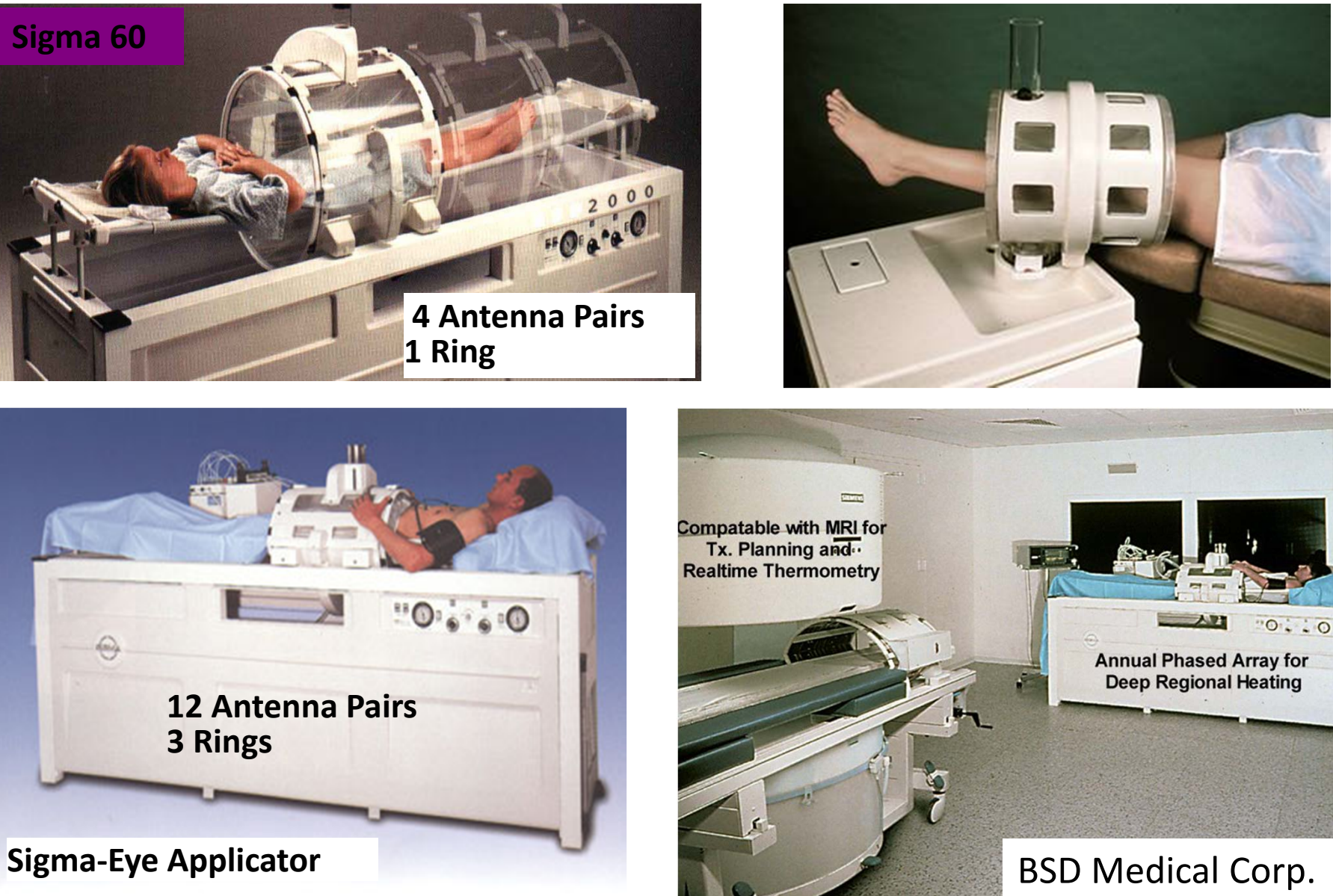


Reitveld & VanRhoon IJH 1999

Samulski, Kapp, Arabe, Jones

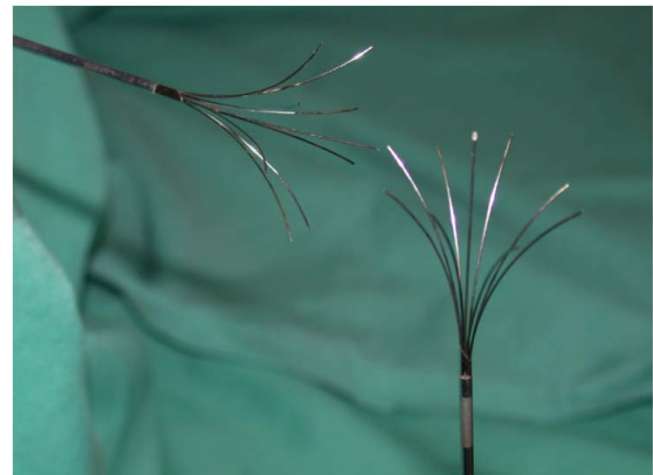
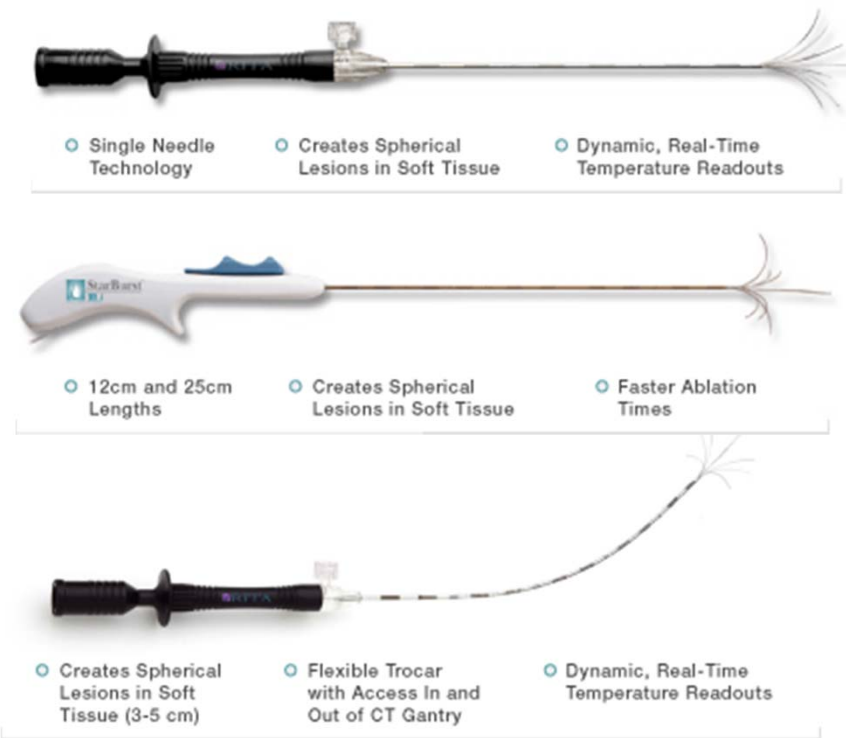


# Annular Phased Array (60 - 120 MHz)



# Commercial RF devices

Monopolar RF devices...cheap and simple



14g/15g trocar

"Starburst" electrodes with integrated temperature sensors (4-9 tines)

# **QUESTION – RF & MICROWAVE HEATING**

# **THERAPEUTIC ULTRASOUND**

# Important Concepts

- Ultrasound interactions with tissue
- Transducer Designs
- Advantages & Challenges
- MRI-guided focused ultrasound
- Clinical examples

# Historical Perspective

- **1950's:** William & Francis Fry (IL) – Development of HIFU for the treatment of Parkinson's disease
- **1980's:** Frank Lizzi (NY) – Development of HIFU for treatment of glaucoma
- **1990's:** Transrectal HIFU for BPH & prostate cancer (France – Lyon, USA – IN) (~10,000 cases)
- **1990's:** Chinese developments – Haifu (Chongqing) (>40,000 cases)

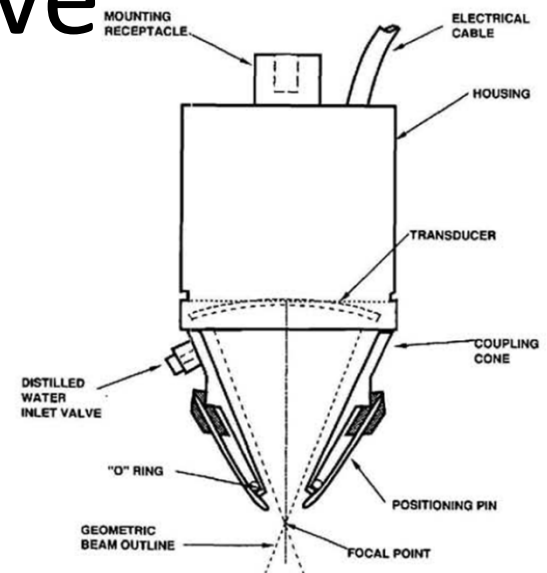
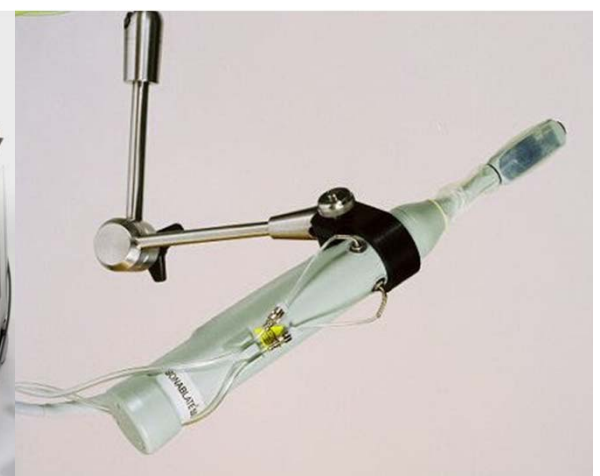


Fig. 1. Schematic diagram of contact therapeutic ultrasound assembly.

Polack et al Invest Opth 32(7), 1991



Focus-surgery.com

# Historical Perspective

- **1990's**
  - MRI-guided focused ultrasound
  - PRF Shift MR Thermometry (1995)
  - Initial studies in uterine fibroids, breast treatments

- **2000's**
  - Insightec (Israel) – Uterine Fibroids FDA Approval
  - Prorhythm – catheter ablation for atrial fibrillation
  - Ongoing trials for bone palliation, breast cancer treatment, prostate, liver, pancreas
  - Cosmetic applications (2009)

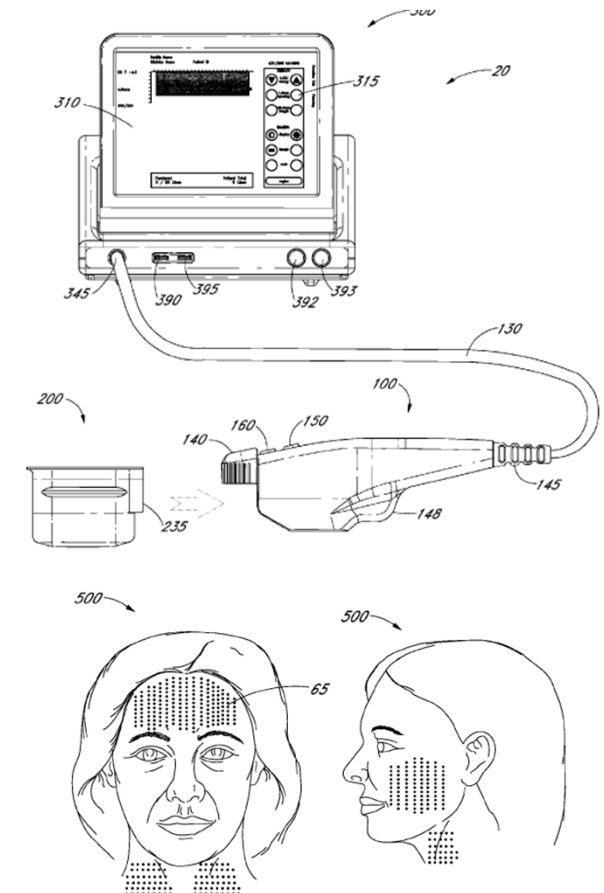
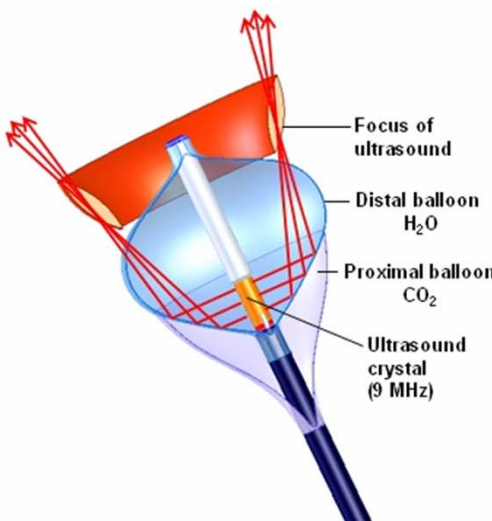


FIG. 12

US 2010/01122405

# Ultrasound Energy

- Speed of sound:  $c = \sqrt{\frac{B}{\rho}}$  ( $\sim 1.5 \text{ mm}/\mu\text{s}$ )
- Frequencies  $> 20 \text{ kHz}$  ( $1 - 10 \text{ MHz}$  for thermal applications)
- Wavelengths in soft tissue –  $0.15 - 1.5 \text{ mm}$
- Compressional wave which results in changes in density & displacement
- Propagation speed in tissues similar to water, but attenuation/absorption quite different

# Some values

**Table 1.5** Amplitudes for a Plane Harmonic Wave propagating in Water at 37 °C for a Time-Averaged Intensity  $\bar{I}$  (W/m<sup>2</sup>) at a Frequency  $f$  (Hz).

Amplitude	Equation	@ 10 mW/cm <sup>2</sup> , 5.0MHz
Pressure, $p_o$	$p_o = 1.734 \times 10^3 \sqrt{\bar{I}}$ Pa	$0.1734 \times 10^5$ Pa
Particle Displacement, $\xi_o$	$\xi_o = 183.7 \times 10^{-6} f^{-1} \sqrt{\bar{I}}$ m	$3.673 \times 10^{-10}$ m
Particle Velocity, $v_o$	$v_o = 1.154 \times 10^{-3} \sqrt{\bar{I}}$ m/s	1.154 cm/s
Acceleration, $a_o$	$a_o = 7.248 \times 10^{-3} f \sqrt{\bar{I}}$ m/s <sup>2</sup>	$3.624 \times 10^7$ cm/s <sup>2</sup>
Fractional Density change, $\Delta\rho/\rho_o$	$\Delta\rho/\rho_o = 7.646 \times 10^{-7} \sqrt{\bar{I}}$	$7.646 \times 10^{-6}$

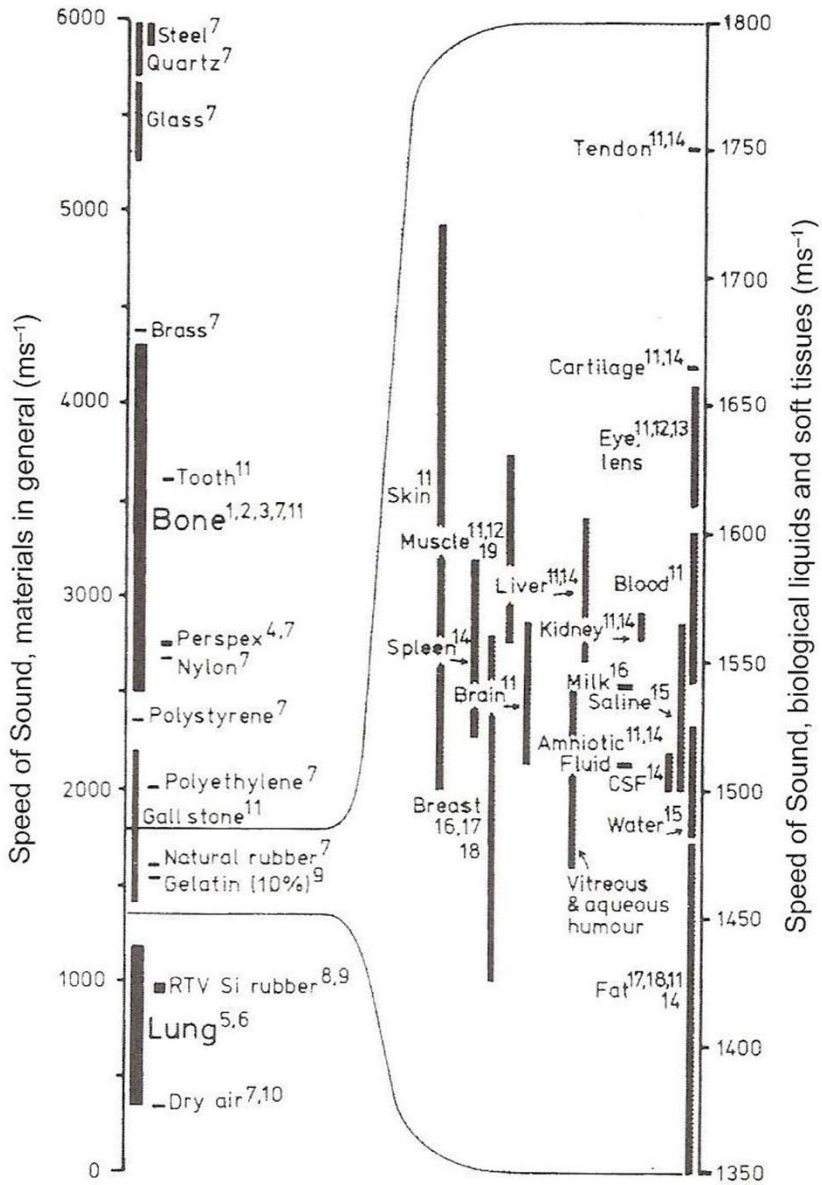
# Acoustic impedance

- Transmission properties determined by acoustic impedance  $Z=\rho c$

$$R_I = \left( \frac{Z_2 - Z_1}{Z_2 + Z_1} \right)^2 \quad T_I = 1 - R_I = \frac{4Z_1 Z_2}{(Z_1 + Z_2)^2}$$

- For water  $z=1.5 \times 10^6 \text{ kg/m}^2/\text{s}$  (Rayleigh)

# Speed of Sound



- $c_{\text{bone}} \gg c_{\text{tissue}}$
- $c_{\text{tissues}} \approx c_{\text{water}}$
- Speed sound is a function of T

# Attenuation

- Gradual loss in intensity of original signal as it passes through a medium

$$d\bar{I}_s = -2\alpha_s \bar{I}(x)dx$$

$$d\bar{I}_a = -2\alpha_a \bar{I}(x)dx$$

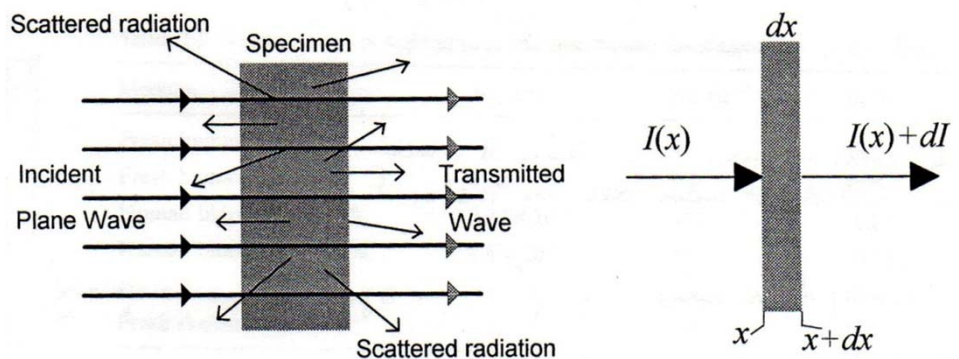
- For the time averaged intensity:

$$\bar{I}(x) = \bar{I}(0)e^{-2\alpha x}$$

where,

$$\alpha = \alpha_a + \alpha_s$$

- Tissue absorption is directly related to protein content
  - i.e. collagen content; very high absorption coefficient



# Attenuation

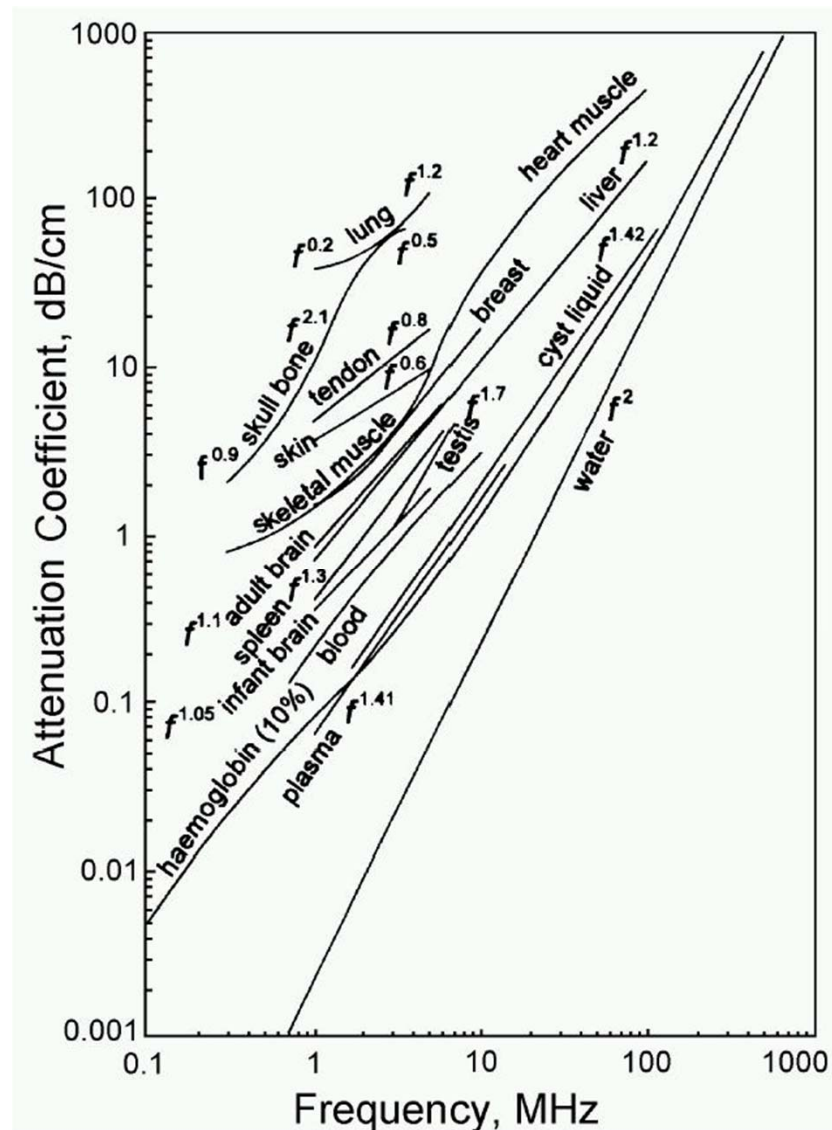
- Attenuation results from scattering and absorption of acoustic wave
- $\mu_{att} = \mu_{abs} + \mu_{scatt}$
- Scattering typically ignored in therapeutic ultrasound modelling
  - Results in simplified calculations
- Attenuation dictates depth of penetration of ultrasound energy, and rate of temperature rise

**Table 1.7.** Contributions of scattering to the attenuation coefficient [1.50].

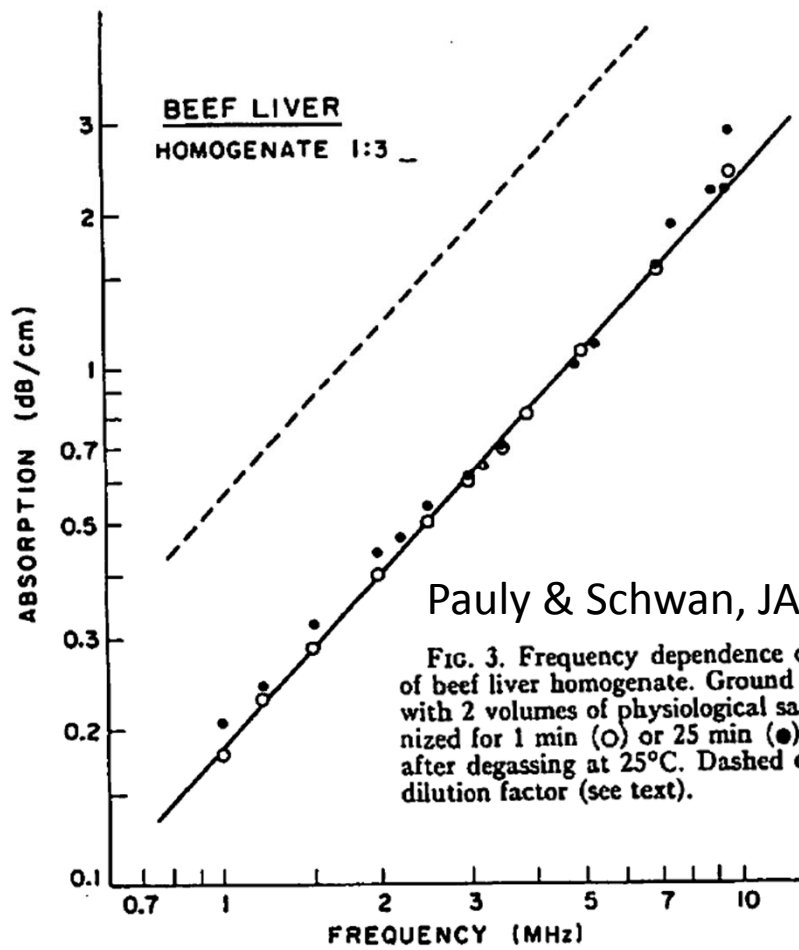
Medium	$2\alpha_s, \text{cm}^{-1}$	$2\alpha, \text{cm}^{-1}$	$\alpha_s/\alpha$	Freq.
Fresh Human Liver	0.09	0.72	12%	4MHz
Fresh Human Liver	0.32	1.4	23%	7MHz
Human Blood, Hct=40%	$0.28 \times 10^{-3}$	0.17	0.1%	4MHz
Human Blood, Hct=40%	$1.8 \times 10^{-3}$	0.37	0.5%	7MHz
Fresh Skeletal Muscle	0.16	0.94	17%	4MHz
Fresh Skeletal Muscle	0.32	1.8	18%	7MHz

# Attenuation

Bamber, 1986



- Frequency dependence:  $\mu_{\text{att}} = \mu_{\text{att}@1\text{MHz}} * f^n$
- Tissues:  $0.2 < n < 1.7$
- Water:  $n = 2$

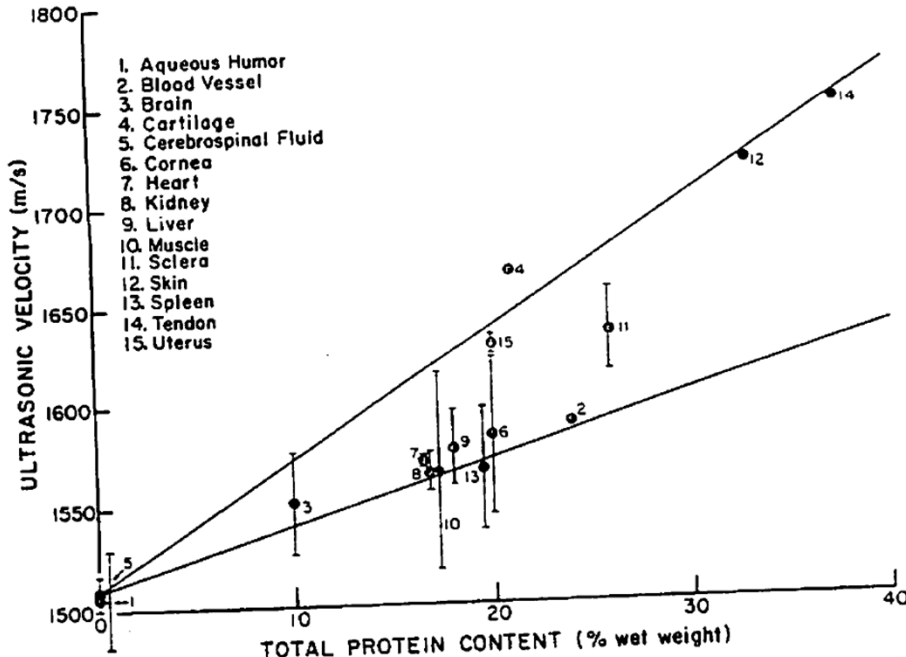


Pauly & Schwan, JASA, 1970

FIG. 3. Frequency dependence of the absorption of beef liver homogenate. Ground liver was diluted with 2 volumes of physiological saline and homogenized for 1 min (○) or 25 min (●) at °C. Measured after degassing at 25°C. Dashed curve corrects for dilution factor (see text).

# Tissue composition

FIG. 1. Dependence of ultrasonic velocity at 1 MHz on tissue proteins. Tissue measurements (•) are compared with the globular protein-free curve (upper curve) and the collagen-free curve (lower curve), both taken from Eq. (1). Standard deviations are indicated for tissues for which several literature values were available. The ranges of protein content are given in Table I.



- Speed of sound and attenuation depend on tissue composition
- Globular (soluble) vs collagen (structural)

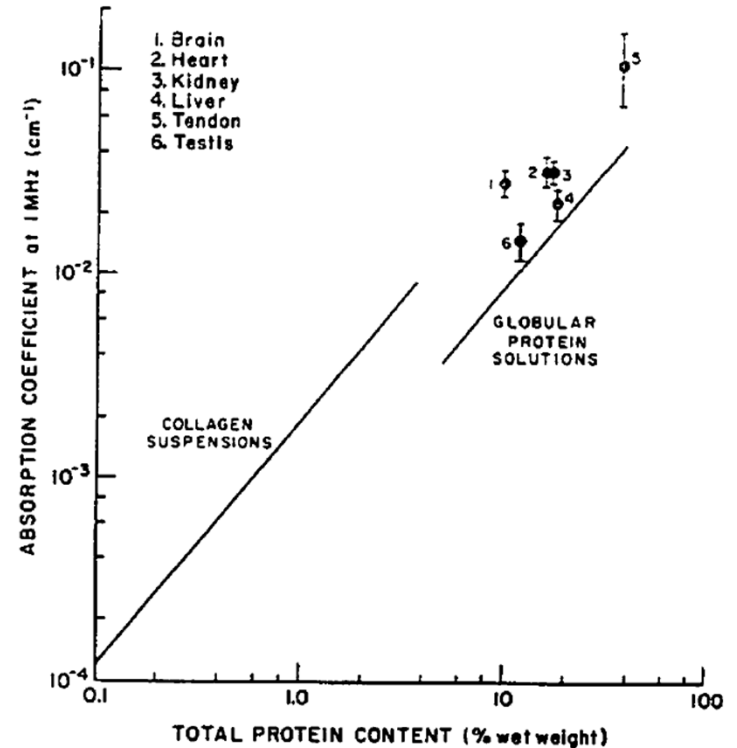


FIG. 2. Dependence of ultrasonic absorption, at 1 MHz on tissue proteins. Tissue measurements<sup>18</sup> (•) appear to fall between the curves defining the ultrasonic absorption of globular protein solutions and of collagen suspensions. The error bars represent the standard deviation. The ranges of protein content are given in Table I.

Goss et al 1980

# Power deposition

- Power deposition given by

$$P = \left( \frac{dI}{dx} \right)_{abs} = 2\alpha_{abs} I_o e^{-2\alpha x}$$

1090

Ultrasound in Medicine and Biology

Volume 21, Number 9, 1995

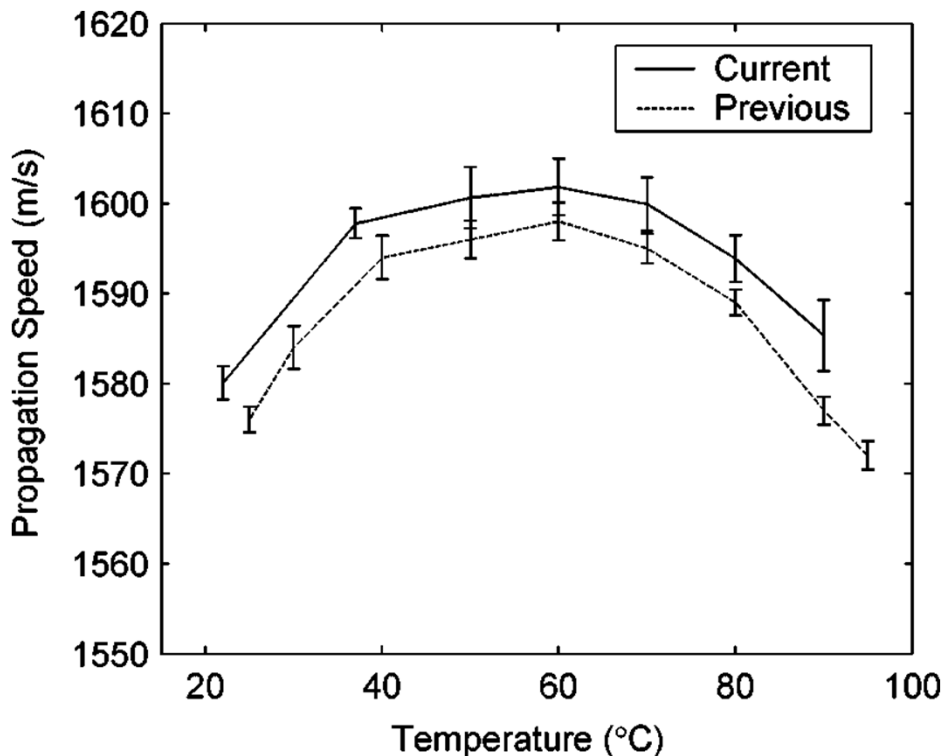
Table 1. Exposure conditions used in typical medical applications of ultrasound.

Application	Typical power	Typical $I_{SPTA}$	Typical pulse length and pulsing regime
Diagnosis			
B-mode	20 mW	$0.017 \text{ W cm}^{-2}$	1- $\mu\text{s}$ pulse; PRF 1 kHz
Pulsed Doppler	60 mW	$1.38 \text{ W cm}^{-2}$	1-10- $\mu\text{s}$ pulse; PRF 10 kHz
Physiotherapy	5 W	$1.5 \text{ W cm}^{-2}$	2-ms pulse; PRF 100 Hz or continuous wave
Surgery	200 W	$1000 \text{ W cm}^{-2}$	0.1-10-s pulse; single exposure

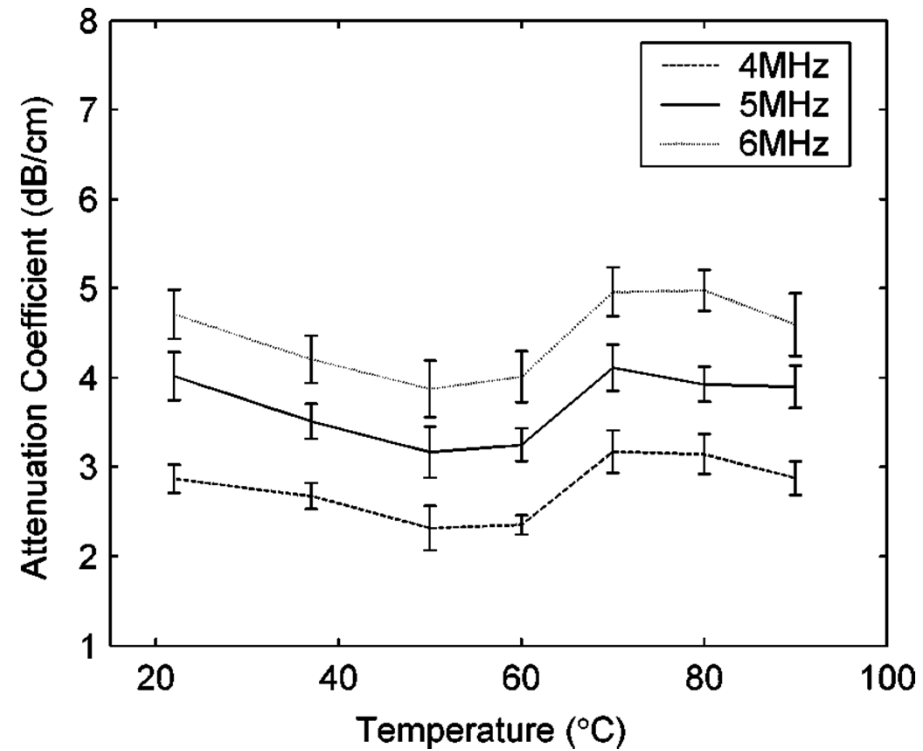
PRF = pulse repetition frequency.

# Temperature Dependence

- Dynamic changes during heating
- $T \sim 100^\circ\text{C}$ : Boiling/vapor formation in tissue occurs
  - Large increase in attenuation (scattering) reduces penetration depth
  - Cavitation can occur



Prop. Speed vs temperature in canine liver



Attenuation vs temperature in canine liver

# Temperature Dependence

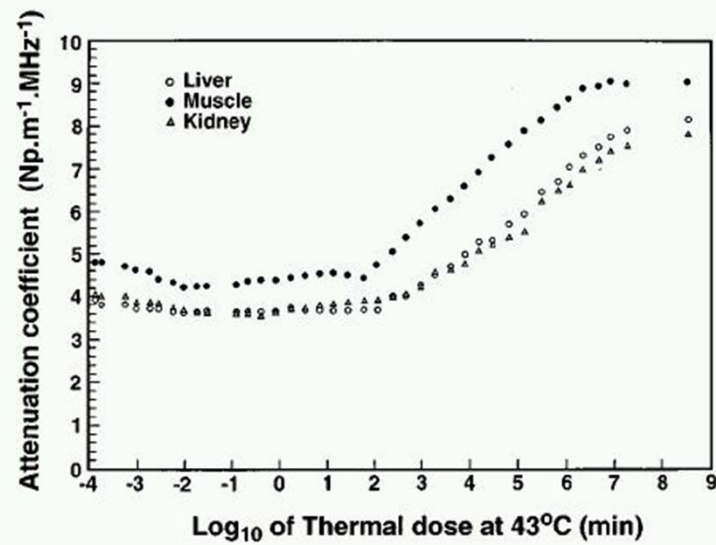


FIG. 5. Attenuation coefficient versus thermal dose at 43 °C for dog muscle, liver, and kidney *in vitro*. Same heating protocol as in Fig. 4.

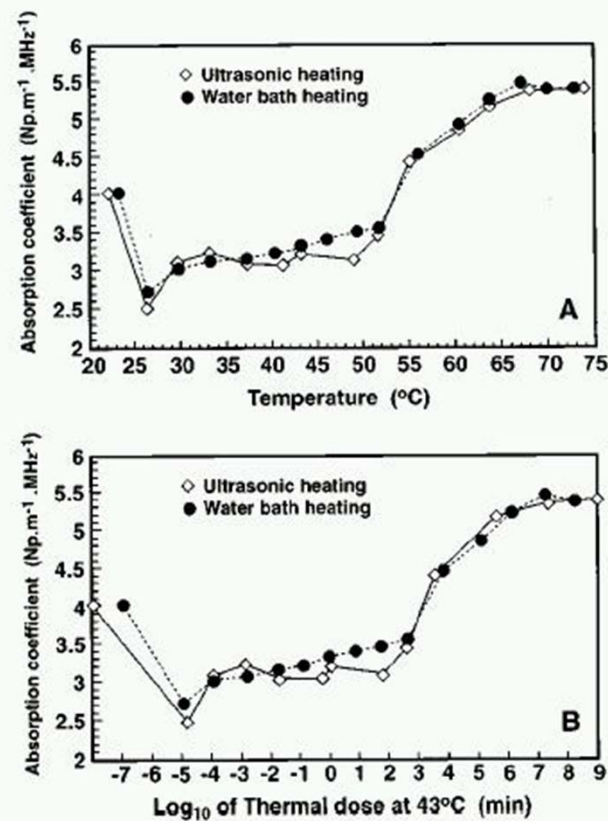


FIG. 7. (A) Absorption coefficient versus temperature (ultrasonically and water bath heated). Dog muscle *in vitro*. (B) Absorption coefficient versus thermal dose.

# Field Calculations

- Scattering ignored, resulting in free field calculation
- Pressure field calculated as a diffraction ir

$$p_o = \frac{j\rho c}{\lambda} \int_S u \frac{e^{-(\mu+jk)r}}{r} dS$$

Rayleigh-Sommerfeld Integral

- Intensity

$$I = \frac{p^2}{\rho c}$$

- Absorbed power  $Q = 2 \alpha I$

- Straightforward for homogeneous medium; more challenging at tissue interfaces (ie bone/soft-tissue) due to impedance mismatch

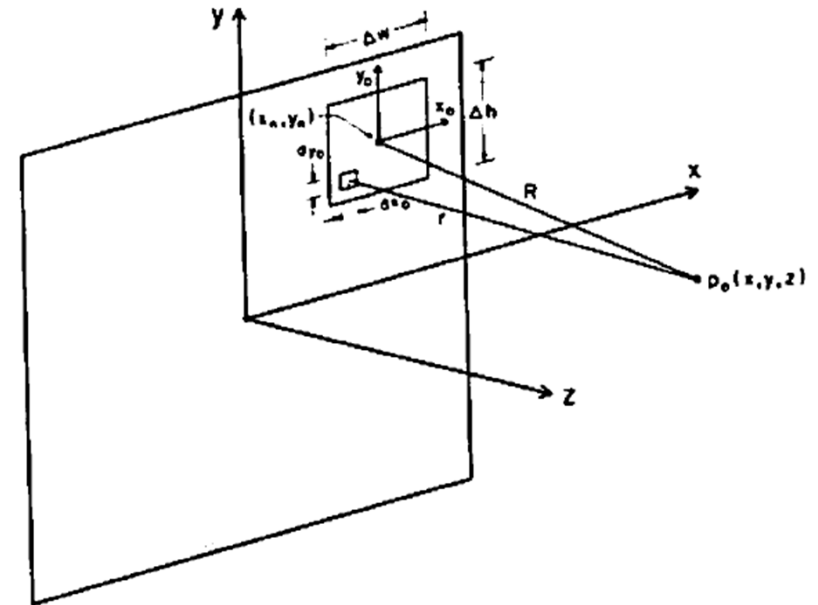


Fig. 1. Coordinate system and geometry used for rectangular radiator method.

# Transducers

## 1. Piezoceramics

- Capable of emitting high power
- Can be shaped in variety of geometries (spherical focusing, cylinders, planar)
- Frequency determined by thickness of ceramic
- Brittle ceramics can be fragile at higher frequencies

## 2. Piezocomposites

- Matrix of epoxy & piezoceramics
- Flexible material capable of forming into various geometries
- Wider bandwidth
- Thermal losses can be limiting factor

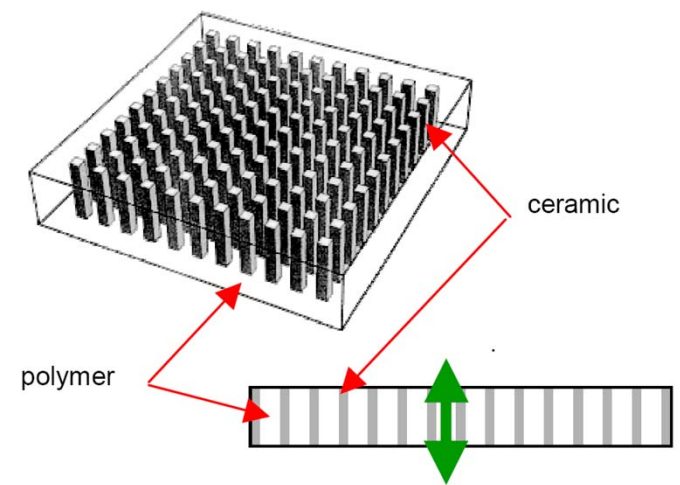
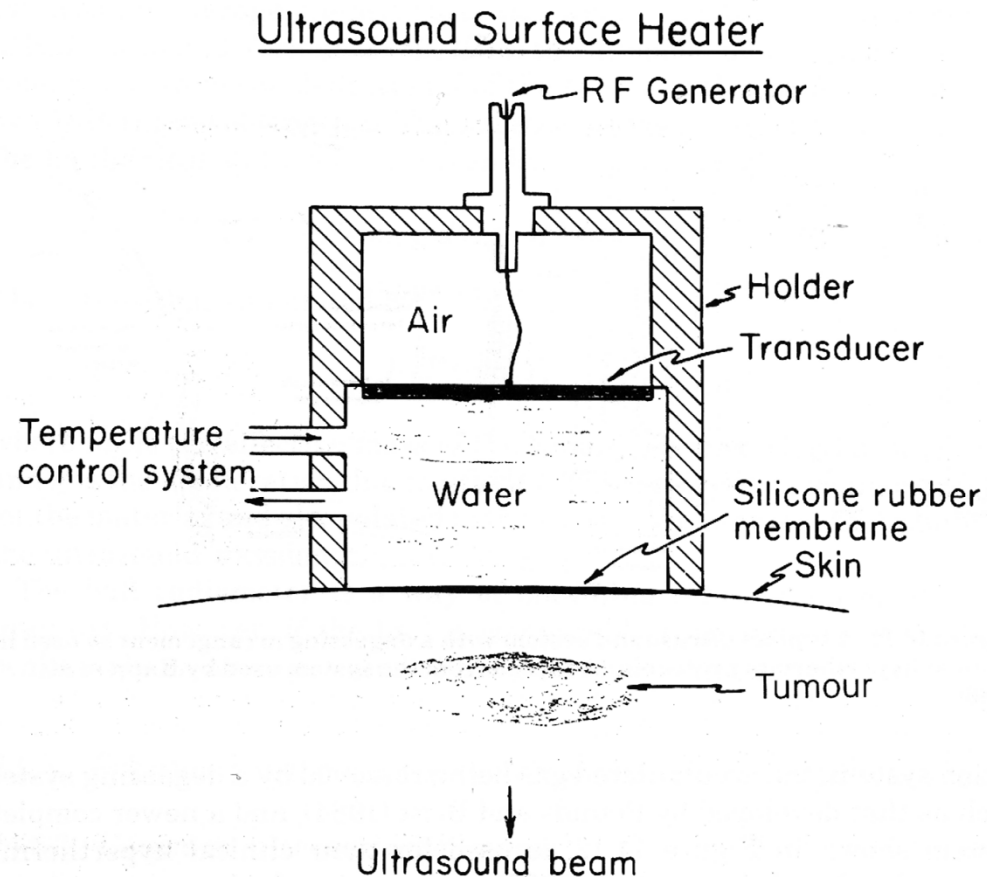


Fig. 1 : 1-3 Piezocomposite after W. A. Smith

# Transducer design



**Figure 14.13** The general principles of a superficial ultrasound heater, with a rapidly flowing, temperature-controlled water cooling system. A coupling medium such as an acoustic gel must be used between the membrane and the skin to eliminate beam loss due to trapped air. (Adapted from Hunt, 1982.)

# Transducers



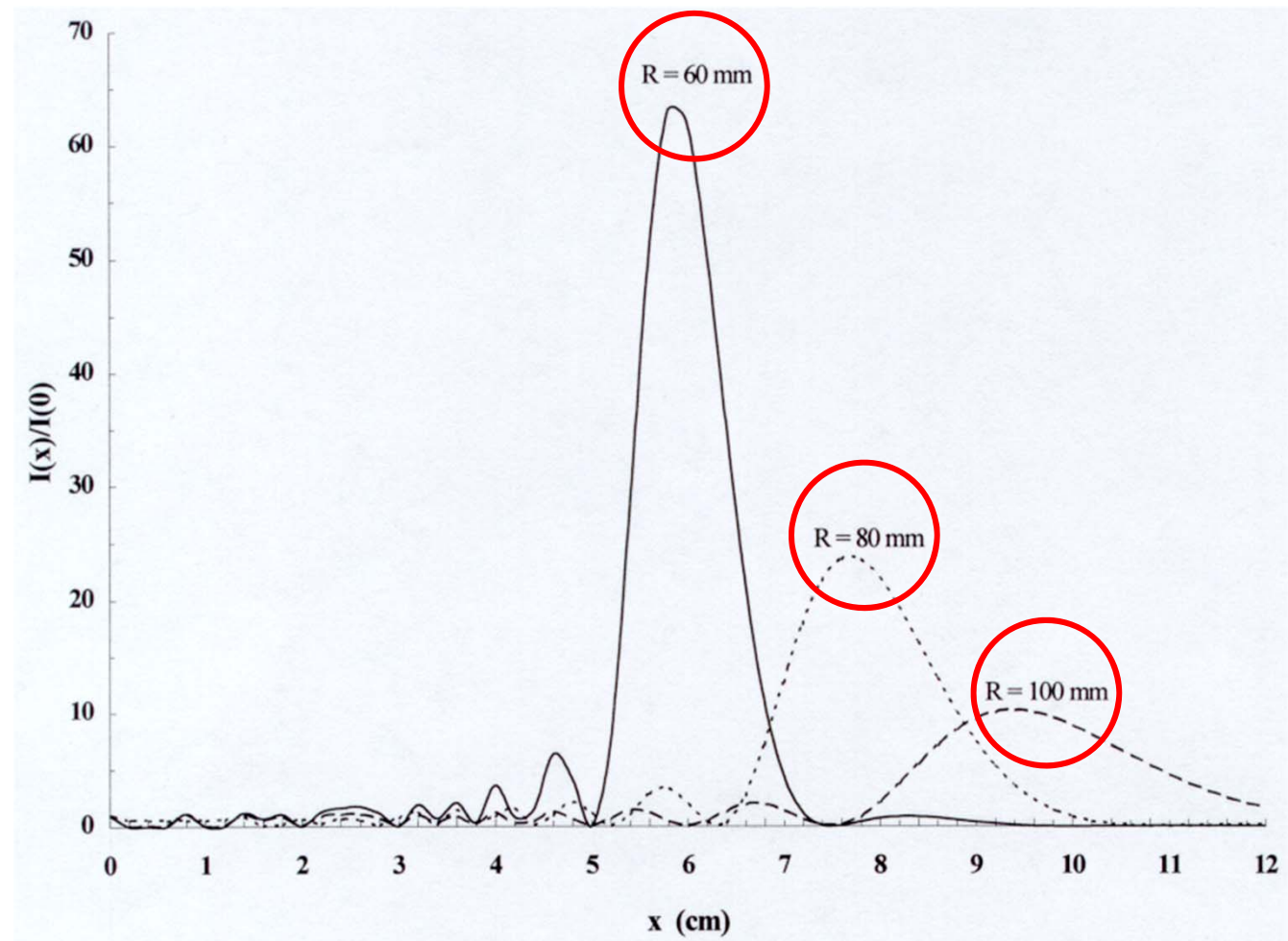
Imasonic, France



# Focused Ultrasound (HIFU)

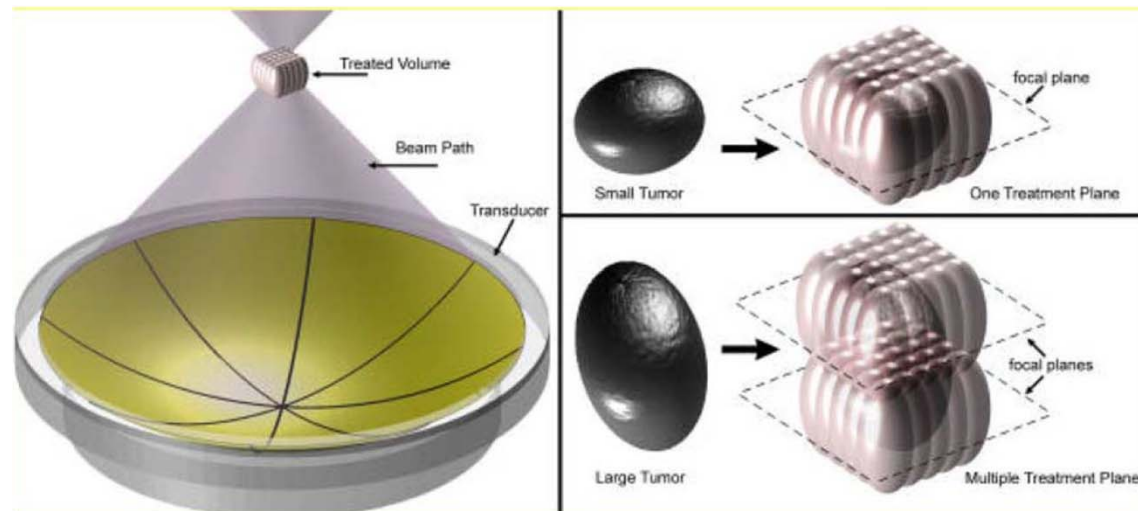
- Can use focused transducers to concentrate acoustic energy to a focal volume at a distance away from the transducer surface

Intensity variation along central axis as function of radius of curvature R  
(1 MHz concave bowl transducer, diameter 60 mm)



# Treatment Strategy

1. Place beam focus within target volume
2. Deposit sufficient energy to coagulate tissue in focal volume (typically seconds)
3. Wait for heat to dissipate in intervening tissues (typically 0.5-1 minute)
4. Translate focus to new location and repeat until entire volume has been covered with focal 'lesions'.



Clement, Ultrasonics 2004



# Features

## Advantages

- Large gain in energy at depth with reduction in intensity in near field
- High spatial precision
  - focal volumes on the order of 1-2mm in diameter, 6-8mm in length
- Non-invasive, rapid energy deposition

## Challenges

- Near field heating
- Treatment time
- Aiming at target within the body...

# Beam Focusing & Translation

## Mechanical

- Simple electronics (typically 1 channel)
- 3D positioning system required to translate beam focus

## Electronic

- Complex electronics (1 -2D phased arrays requiring hundreds of channels with control over amplitude & phase)
- Rapid scanning of volume possible due to electronic switching
- Elimination of mechanical components reduces profile of device
- ***Can also generate more sophisticated beam shapes than single focal spots***

# A study of various parameters of spherically curved phased arrays for noninvasive ultrasound surgery

Xiaobing Fan† and Kullervo Hynynen

Department of Radiology, Brigham and Women's Hospital, Harvard Medical School, Boston, MA 02115, USA

Phys. Med. Biol. 41 (1996) 591–608.

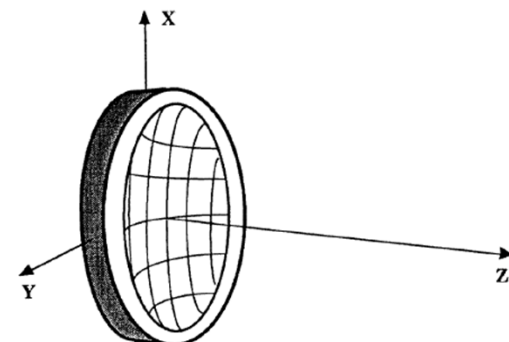


Figure 1. A diagram of the phased array design and the coordinate system used in this study.

- Theoretical study investigating the important parameters influencing treatment of a 3x3x3 cm volume of tissue

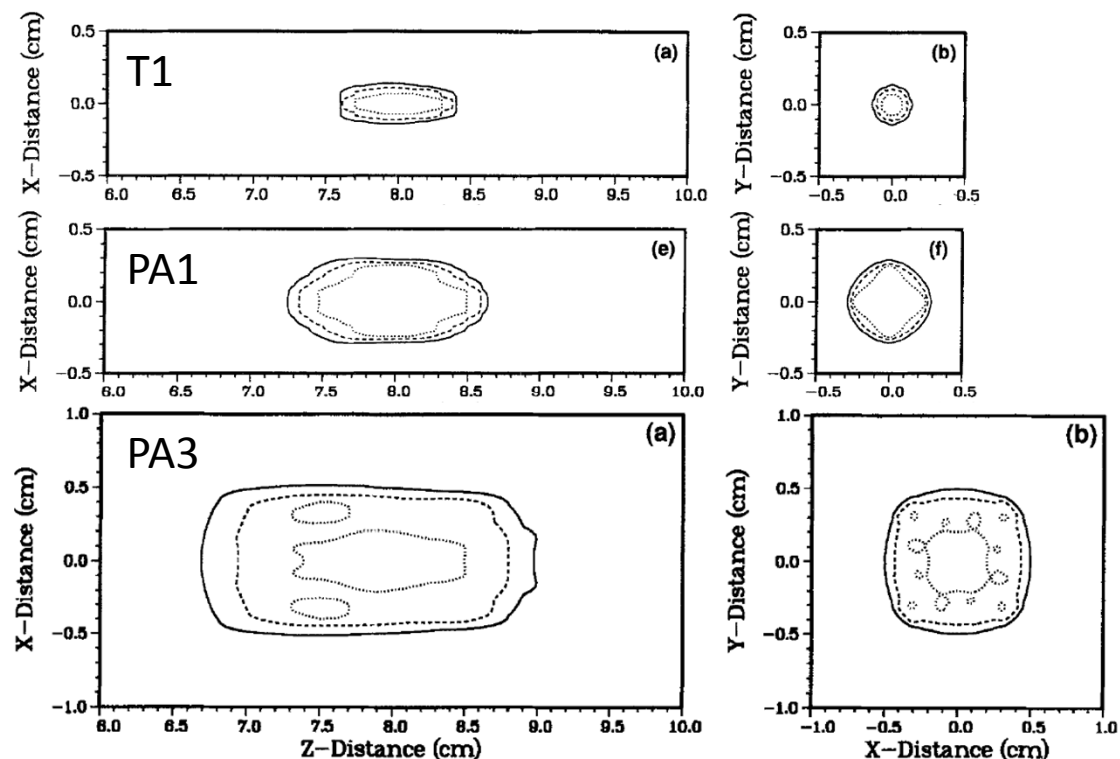


Fig. 2. The lesion boundary (isothermal dose at 240 min at 43°C) for three different pulse durations: 10 s (solid line), 5 s (dashed line) and 1 s (dotted line). The transducers used in the simulations are given in Table 2: for

# Treatment time & volume

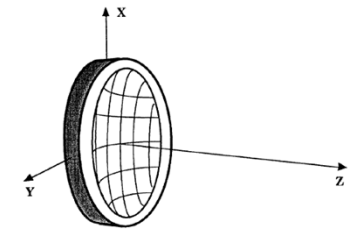


Figure 1. A diagram of the phased array design and the coordinate system used in this study.

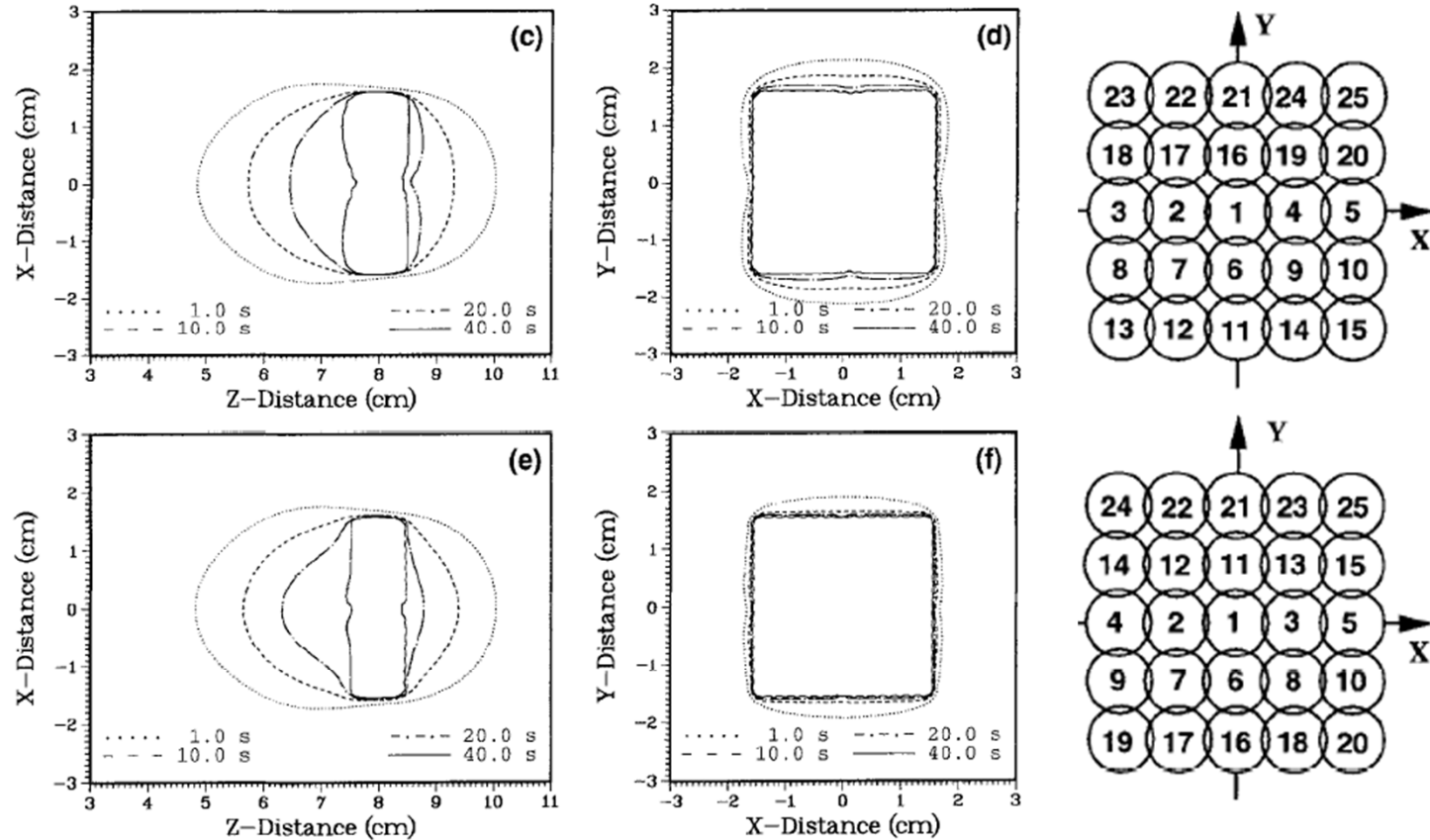


Fig. 5. The effects of transducer movement on the necrosed tissue volume: (a, b) one-sided; (c, d) two-sided; and (e, f) alternated. The transducer T1 was used in the calculations with a 10-s pulse duration and four different delay times (1-s, dotted line; 10-s, dashed line; 20-s, chained line; and 40-s, solid line). The figures on the left are axial plane distributions, and those on the right are focal plane distributions.

# Treatment time & volume

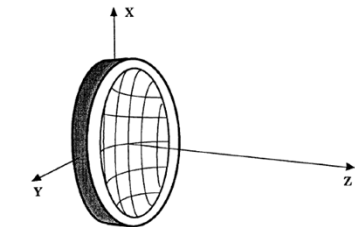


Figure 1. A diagram of the phased array design and the coordinate system used in this study.

Table 4. The ultrasound pulse durations, delay times, number of pulses in each focal plane and number of focal planes used in the simulations (input power for each case is given in Table 3).

Transducer	Pulse duration (s)	Delay time (s)	Number of pulses and planes	Treatment time (h)	Rate of necrosed tissue (cm <sup>3</sup> /h)
<i>T1</i>	10	40	225	12.5	2.4
	5	30	400	15.5	1.7
	1	14	900	22.5	1.2
<i>T2</i>	10	120	144	10.3	3.9
	5	90	225	11.8	3.4
	1	44	400	10.0	3.0
<i>PA1</i>	10	130	49	3.8	8.5
	5	100	49	4.3	7.3
	1	69	81	4.7	6.3
<i>PA2</i>	10	460	25	3.1	9.6
	5	390	36	3.8	7.2
	1	309	64	10.9	5.1
<i>PA3</i>	10	440	16	3.9	14.6
	5	320	16	2.8	11.6
	1	—	—	—	—

The 64-element phased array with radius of curvature 15 cm is not used in the treatment simulations.

# Thermal lensing

- Related to temperature dependent speed of sound in tissues
- $C_{\text{fat}}$  decreases with temperature
- $C_{\text{tissue}}$  increases with temperature

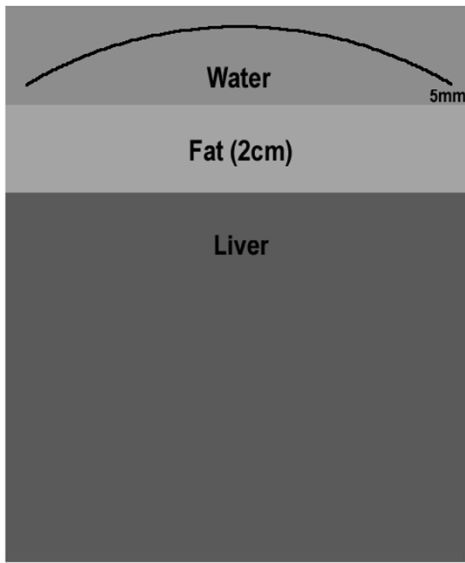


Figure 1. Arrangement of tissues and the sector vortex array.

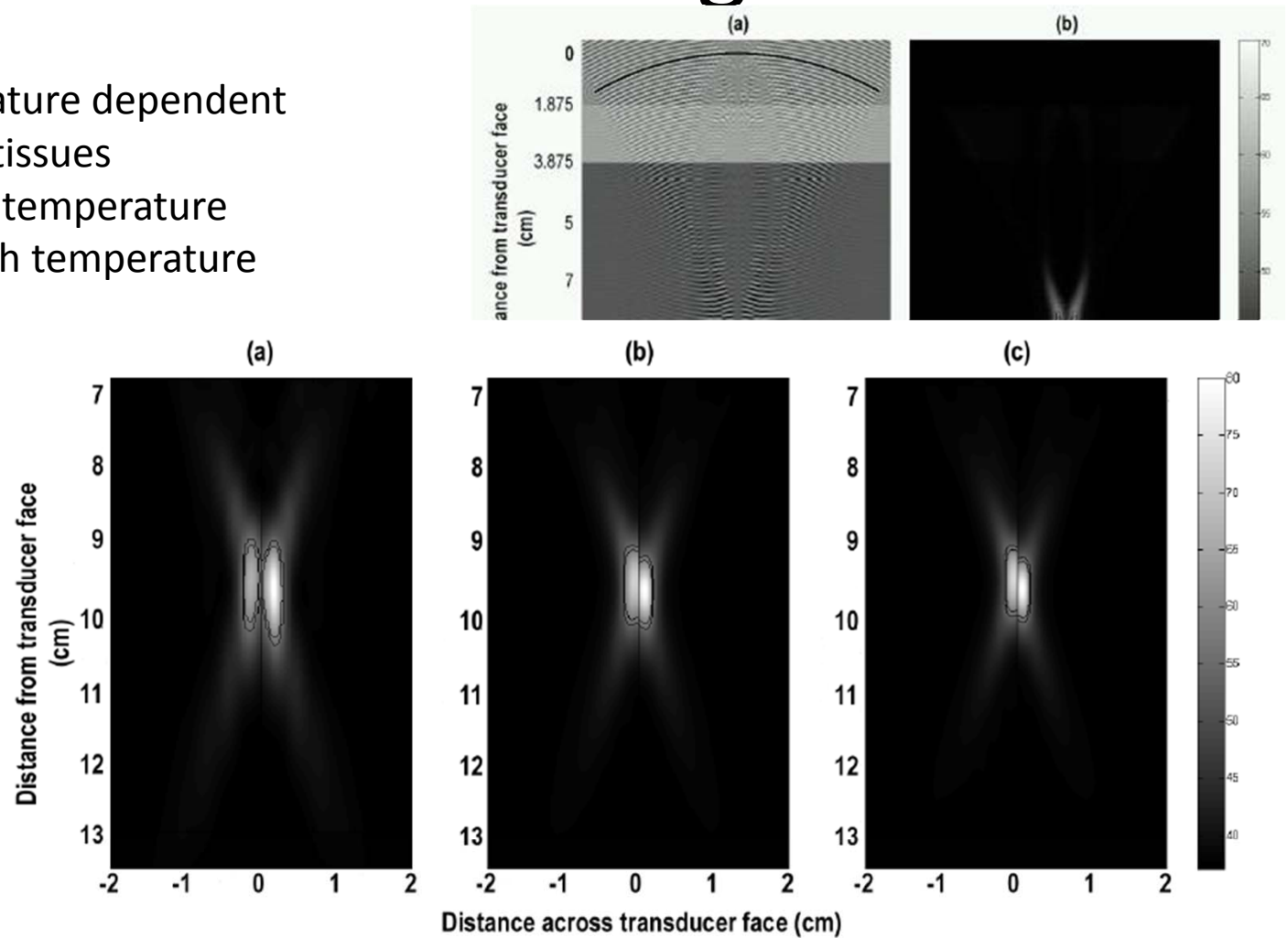


Figure 5. Thermal fields under sonication at 666 kHz, 1 MHz and 1.2 MHz. (a) Mode 1, 666 kHz,  $f$ -number 1.0. (b) Mode 1, 1 MHz,  $f$ -number 1.0. (c) Mode 1, 1.2 MHz,  $f$ -number 1.0. The left half-planes are without thermal lensing while the right half-planes are with thermal lensing.

# Harmonic generation

- Pressure wave becomes non-linear with increasing amplitude and distance travelled
- Implications for therapy?

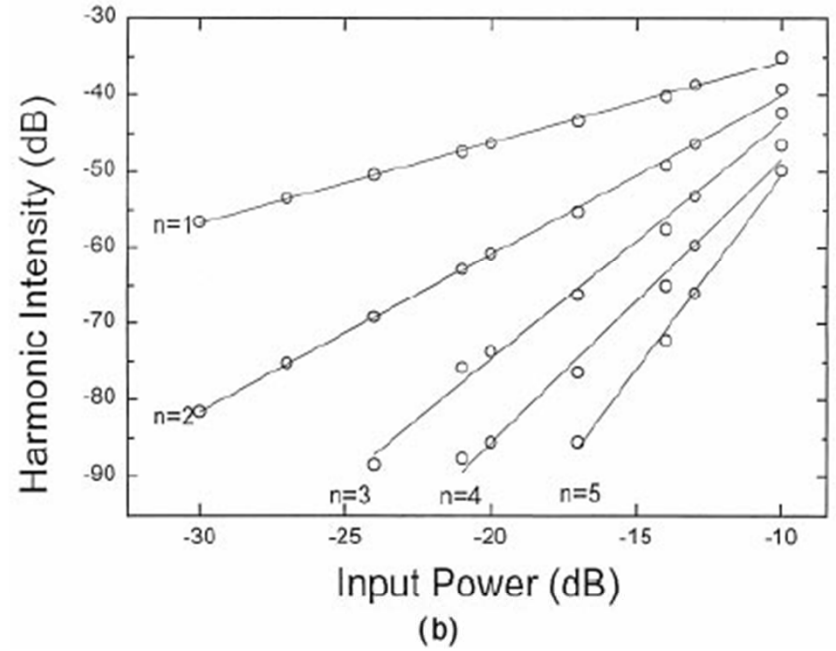
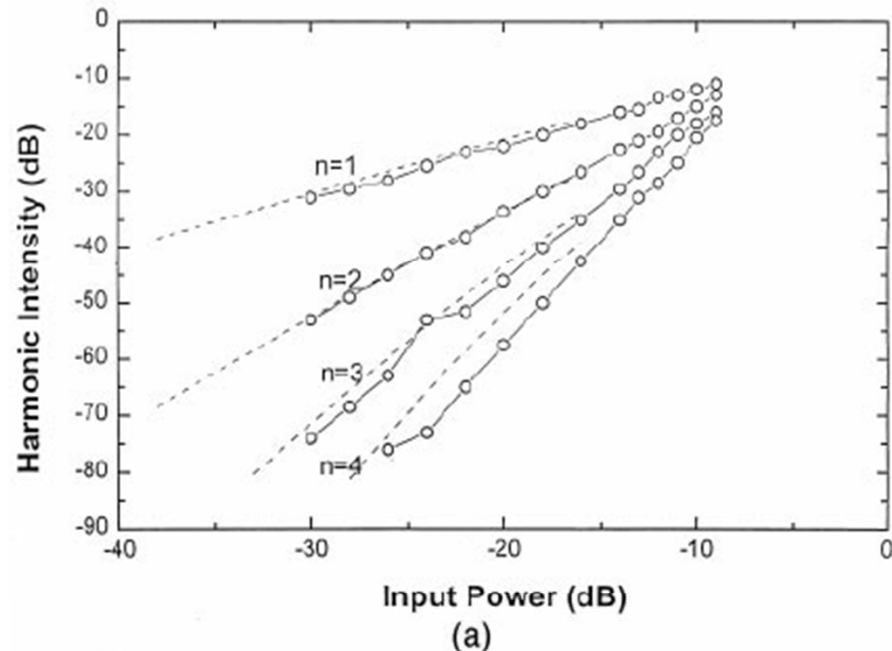


Fig. 2. Harmonic generation in liver, at the focus. (a) First series, (—) experiment; (—) theory. (b) Second series, (○) experiment; (—) least squares fits. Harmonics range from 1 to 4 (Series 1) or 5 (Series 2) from top to bottom. The numbers on the curves indicate the harmonic number. The reading errors are on the order of  $\pm 1$  dB.

# Non-linear effects on HIFU

- Due to the pressure-induced changes in density

$$c = \sqrt{\frac{B}{\rho}}$$

- Results in enhanced heating, and tightening of the focal volume in HIFU

Connor et. al. Phys. Med. Biol. **47** (2002) 1911–1928

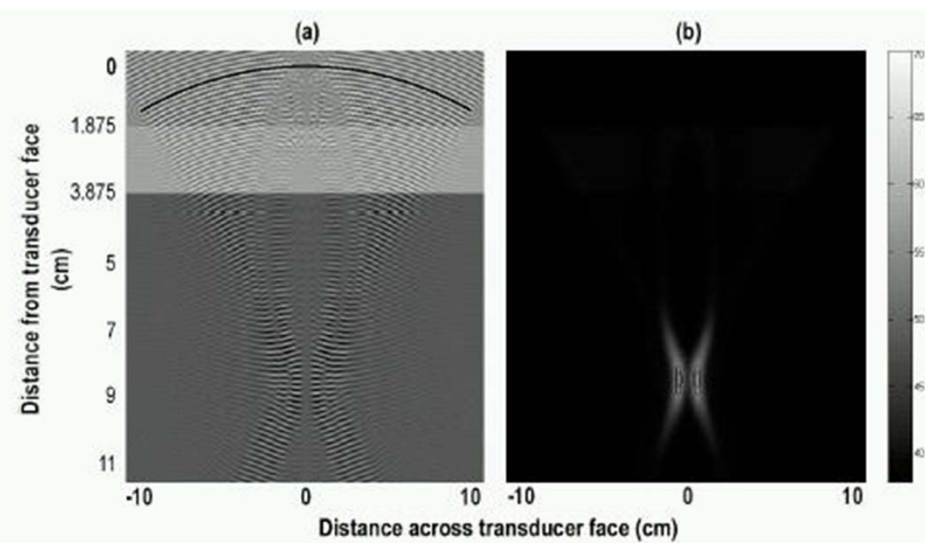


Figure 8. Simulation of mode 4 sonication at 1 MHz with classical linear theory. (a) Pressure field produced by classical methods. (b) Temperature field produced by classical methods.

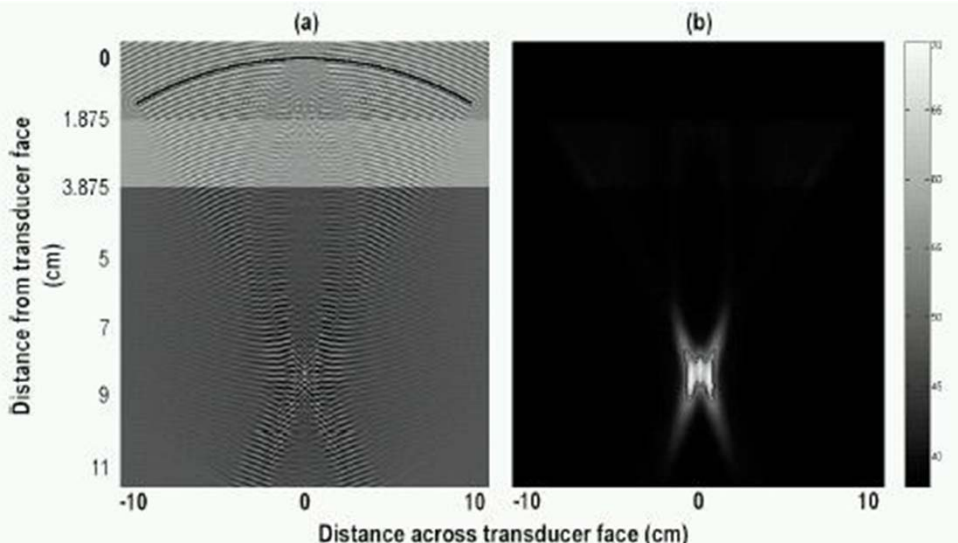


Figure 9. Simulation of mode 4 sonication at 1 MHz with nonlinear theory. (a) Pressure field produced by nonlinear methods. (b) Nonlinear temperature field produced by nonlinear methods.

# MRI-guided focused ultrasound

- First paper in 1992 (Cline et al)
- Prototype systems developed at GE Research and distributed
- Substantial improvements made in academic labs
- Initial systems incorporated mechanically-scanned single element transducers
- Next generation systems incorporated phased array transducers
- Insightec formed (significant ownership by GE) to develop MRI-guided focused ultrasound clinical systems (breast, uterine fibroids, bone, prostate, brain)
- Currently about 50 systems around the world used to treat uterine fibroids
- Other MRI vendors are developing MRI-guided focused ultrasound technologies (Philips, Siemens)

# Clinical Example

- MRI-guided focused ultrasound surgery of breast fibroadenoma (Hynynen et al, 2001)
- 9 patients treated prior to surgery

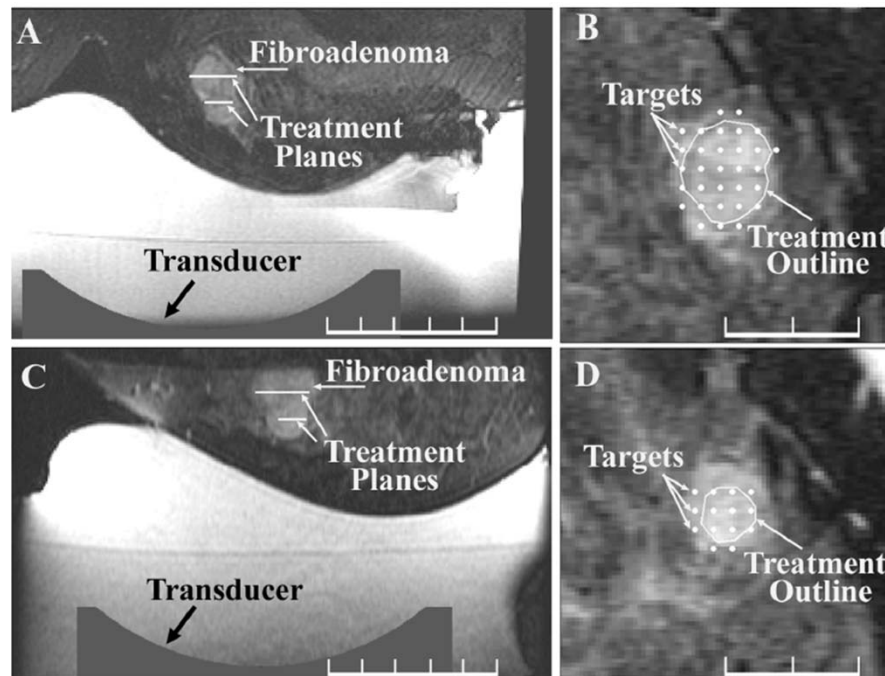
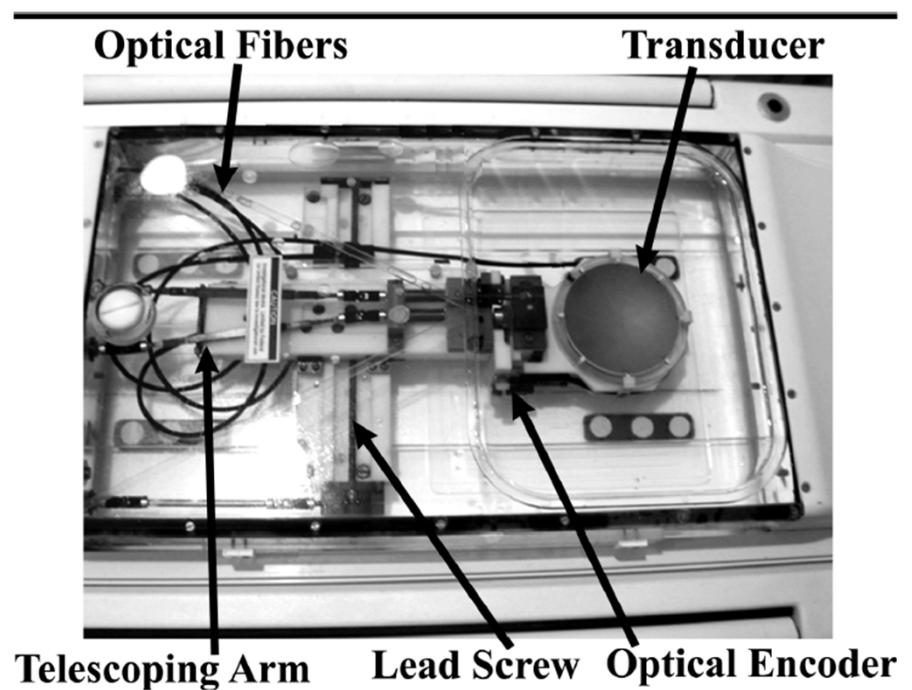


Figure 2. Fat-suppressed T2-weighted fast SE MR images (2,500/100) obtained for planning on the day of treatment of a fibroadenoma. The patient is lying in a prone position, with the breast positioned on the water pillow. The transducer is outlined at the bottom. Transverse sections (A, C) and the corresponding coronal sections (B, D) of the planning target volume outlined in two sequential planes are shown. The positions of the treatment foci are demonstrated in B and D.



# Clinical Example

- MRI-guided focused ultrasound surgery of breast tissue

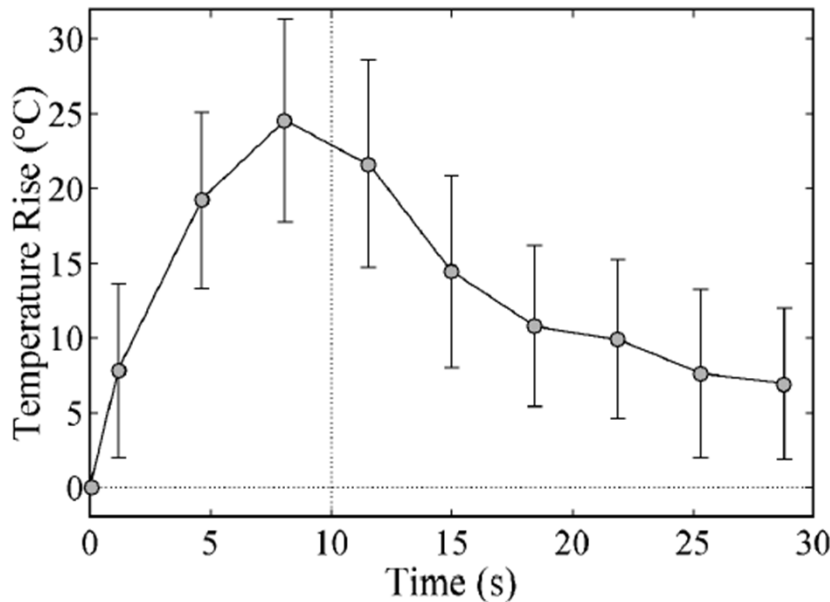


Figure 4. Graph shows mean temperature elevation as a function of time of the hottest voxel of 63 sonifications delivered to a breast fibroadenoma, as measured with MR imaging-derived thermometry. The temperature increase was  $17.5^{\circ}\text{--}45.2^{\circ}\text{C}$ . A total of 71 sonifications in three planes were delivered to this tumor. Temperature increase could not be reliably monitored in eight sonifications because of noise on the images, which was induced by fatty tissue surrounding the tumor.

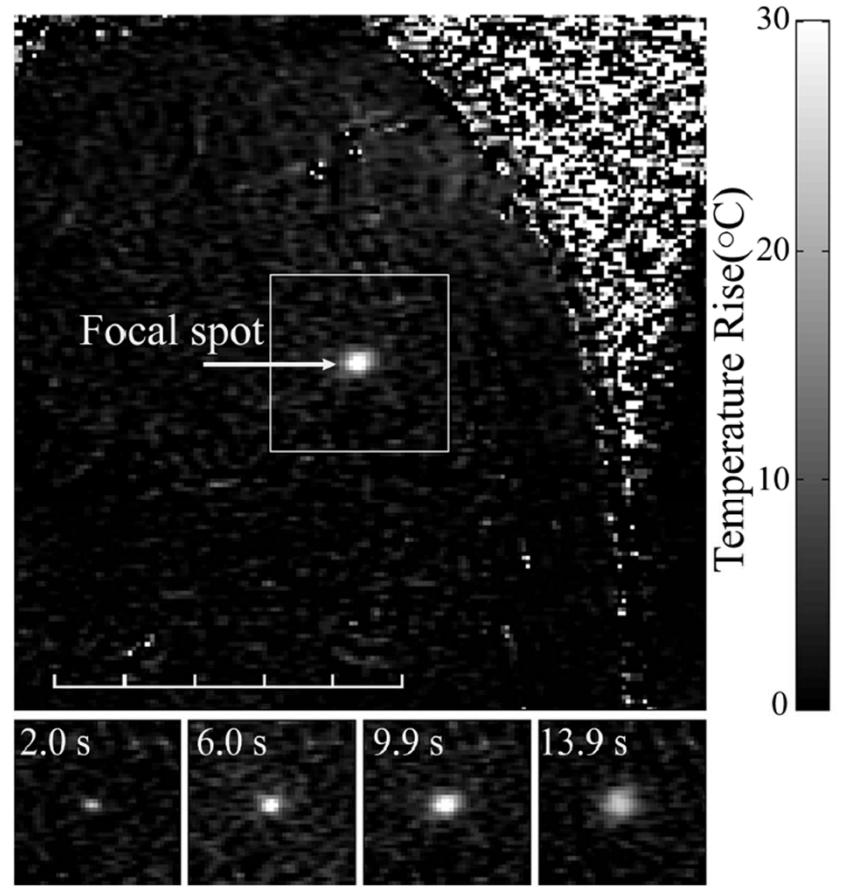


Figure 3. Temperature-sensitive fast spoiled gradient-echo phase-subtraction MR images (27.3–13.5) of a single 10-second therapeutic sonication in the tumor. Top: MR image shows the temperature elevation at the end of a sonication during therapy in the tumor in Figure 2, A, with proton resonance frequency imaging. The temperature focus appears as a small hyperintense spot in the breast. Bottom: MR images show the temperature time-course of the same sonication in the

# Clinical Example

- MRI-guided focused ultrasound surgery of uterine fibroids (Tempany et al 2003)
- Nine patients underwent non-invasive thermal coagulation of a volume within an existing fibroid, prior to surgery
- Only a single plane was treated

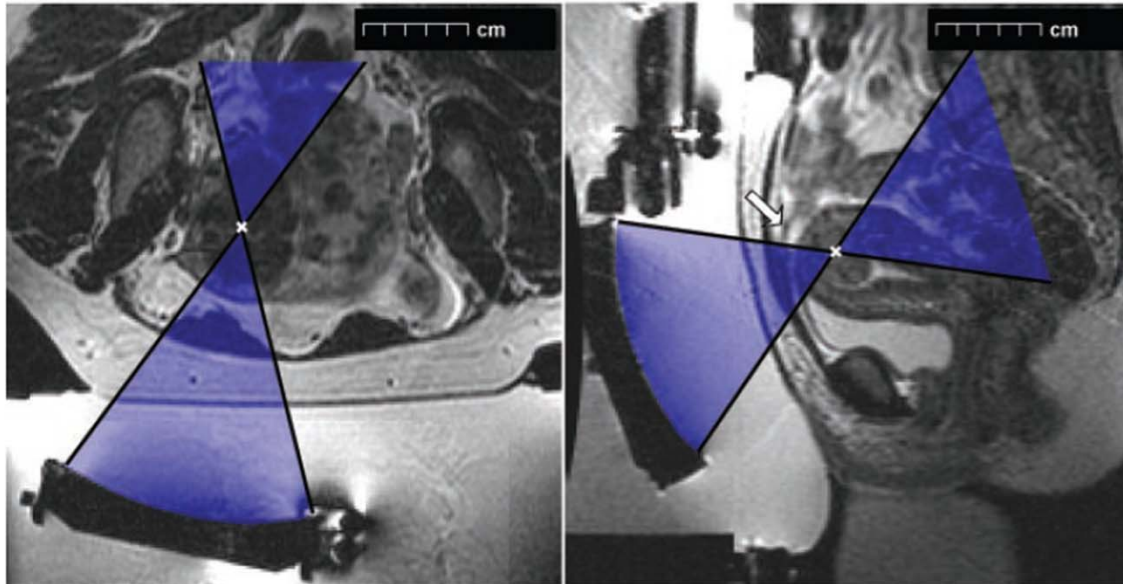


Figure 2. Patients 3 and 4. Transverse (left, patient 3) and sagittal (right, patient 4) T2-weighted fast SE MR images (2,500/98) with the patient in position for ultrasound surgery of uterine fibroids. In these cases, the transducer was angled during the treatment. The arrow on the right indicates the bowel loop that was avoided by angling the transducer.

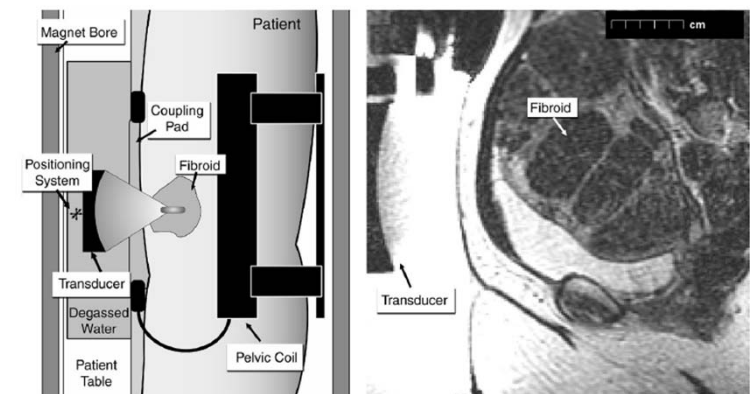


Figure 1. Patient 2. Left: Side-view diagram of the focused ultrasound system and patient positioning. Right: Sagittal T2-weighted fast SE MR image (repetition time msec/echo time msec = 2,500/98) obtained with the patient in position for treatment.

# Clinical Example

Room time: 3h19 – 4h55

Treatment time: 1h – 2h32

Sonication time: 0.5 – 2h15

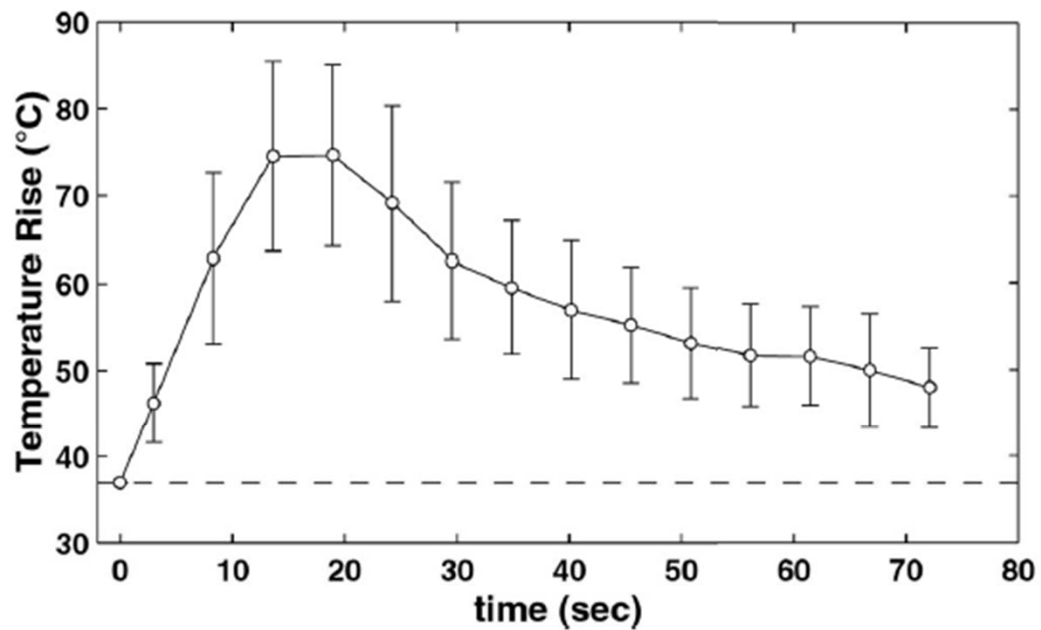


Figure 6. Patient 8. Line graph depicts temperature measured at the focus for 23 sonication in one treatment. The focal temperature increase was sufficient to cause thermal damage in each case. The variation from location to location was significant. Error bars = SD, dotted line = baseline body temperature ( $37^{\circ}\text{C}$ ).

